

GODAE inter-comparisons in the Tasman and Coral Seas

PR Oke¹, GB Brassington², J Cummings³, M Martin⁴, F Hernandez⁵

¹The Centre for Australian Weather and Climate Research (CAWCR), Commonwealth Scientific and Industrial Research Organisation (CSIRO), Hobart, Australia

²CAWCR, Bureau of Meteorology (BoM), Melbourne, Australia

³Naval Research Laboratory (NRL), Monterey, USA

⁴Met Office, Exeter, UK

⁵Mercator Ocean, Ramonville, France

This paper compares the performance of operational short-range ocean forecast systems developed under the Global Ocean Data Assimilation Experiment (GODAE) – an international effort to demonstrate the feasibility of operational ocean forecasting. ‘Best estimates’ from four different operational forecast systems (either analyses, hindcasts, or nowcasts) are inter-compared for the Tasman and Coral Seas, off eastern Australia. Systems considered include those developed in Australia, France, the USA, and the UK. Each system is compared to observations of along-track sea-level anomaly, sea-surface temperature, near-surface velocity, and sub-surface temperature and salinity. All have their strengths and weaknesses, and each system out-performs all others in one aspect or another. With few exceptions, all systems demonstrate signal-to-noise ratios greater than one for all variables. Due to the Australian focus, in addition to the best estimates from the operational systems, operational forecasts and a delayed-mode reanalysis are also inter-compared using the Australian system. The Australian system generally performs the best for sea-level anomaly; the French system is best for near-surface velocities; the USA system generally performs the best for sea-surface temperature; and the UK system is best for sub-surface temperature and salinity. These findings provide useful indicators of deficiencies in each system and clear metrics by which future developments should be assessed. Based on these results and other practical considerations the adoption of multi-model consensus forecasting, using all available forecasts from all systems, is promoted as the most robust approach for the user community. Such developments are being pursued under GODAE OceanView – the successor to GODAE. The results show the success of GODAE in demonstrating the feasibility of operational oceanography.

LEAD AUTHOR'S BIOGRAPHY

Peter Oke is a Research Scientist at the Commonwealth Scientific and Industrial Research Organisation (CSIRO). He leads the ocean data assimilation and ocean modelling teams in the Bluelink Project, and is Co-Chair of the GODAE OceanView task team on Observing System Evaluation.

INTRODUCTION

The primary goal of the Global Ocean Data Assimilation Experiment^{1,2} was to demonstrate the feasibility of operational ocean forecasting. Additional goals included the development and application of state-of-the-art ocean models and data

assimilation methods for short-range open-ocean forecasts; the provision of global ocean analyses and reanalyses for developing and improving understanding of the oceans; improving assessments of the predictability of ocean systems; and improving the design and effectiveness of the global ocean observing system.

Several data-assimilating ocean modelling systems have been developed under GODAE and are used for operational ocean forecasting and ocean reanalysis on either regional or global scales.^{3,4} These include Bluelink from Australia;^{5,6,7} FOAM from the UK^{8,9}; HYCOM from the USA^{10,11}; Mercator from France;¹² TOPAZ from Norway;¹³ MOVE and COMPASS-K from Japan;¹⁴ C-NOOFS from Canada (www.c-noofs.gc.ca/); and the ECCO group (www.ecco-group.org). All these systems are unique – in most cases using different model codes, different model resolution, different domains, different parameterisations, different observation sources, different surface forcing, and different data assimilation methods.

Prior to the final GODAE Symposium (www.godae.org/Final-GODAE-Symposium.html), in November 2008, an internationally coordinated effort to undertake model inter-comparisons of the operational ocean forecast systems was undertaken. Results¹⁵ focussed on the North Atlantic, tropical Atlantic, and North Pacific basins. They concluded that the ocean dynamics of all systems were consistent; that the wind-driven circulation was satisfactorily represented by all systems considered; all systems reasonably represented the thermohaline circulation. There were differences in the representation of the eddy-scale variability and further analysis is required to understand these differences.

These activities did not include a detailed inter-comparison with the Australian system, because the Australian system lacks sufficient resolution in the focus regions of that study. It is noted that the diversity of physical oceanography in the Australian region that is chosen for this study is particularly interesting for assessing GODAE systems. It includes a western boundary current, with intense currents, fronts, and evolving (propagating) features, strong horizontal gradients, and non-linearities. All these features pose significant challenges for models and assimilation schemes, particularly where observations only marginally resolve the features of interest.

The region considered here also includes a tropical area, the Coral Sea, where vertical stratification and fast-propagating dynamics are often difficult to reproduce with models. Finally, the coastal areas considered in this study also permit some possible insights into how well each system represents the slope and shelf dynamics, and its interactions with open ocean processes.

The primary motivations for this paper are two-fold: firstly, to extend the inter-comparisons¹⁵ to the Australian region, and to include comparisons with the Australian system; secondly, to quantify the performance of GODAE systems at the end of GODAE in 2008, by comparing each system to observations. Notably, developments on GODAE systems continue under GODAE OceanView (www.godae-oceanview.org), the successor to GODAE.

The remainder of this paper includes a brief description of the models and assimilation systems, a comparison of the products, the results and a discussion of the inter-comparisons, and finally the conclusions.

SYSTEM DESCRIPTIONS

The important elements of the models and assimilation systems used in the forecast systems are presented in Table 1. Detailed descriptions of each assimilation system are available in published literature,^{7,9,10,16} including summary papers that contrast all assimilation and model systems.^{3,4,17} The descriptions that follow are focussed on identifying the differences between the systems that may explain differences in the results, shown later. These descriptions only include those aspects directly relevant to the specific versions of each system that were used for the final GODAE inter-comparison exercise. However, it is noted that development on each system continues.

Model overview

Of the systems shown in Table 1, Bluelink (Australia) and HYCOM (USA) are eddy-resolving in the region of interest (1/10° and 1/12° respectively), and FOAM (UKMet) and Mercator (French) are eddy permitting (both 1/4°). Bluelink, FOAM and Mercator all use z-level models, while HYCOM uses a hybrid, adaptive vertical grid (www.hycom.org). Both FOAM and Mercator use the same model code and grid (NEMO; www.nemo-ocean.eu/). Bluelink uses MOM4.¹⁸ All systems use different in-house or national numerical weather prediction (NWP) flux products. The heat and freshwater fluxes for Bluelink and FOAM include diurnal variability, while Mercator and HYCOM use daily averaged heat and freshwater fluxes. Similarly, the wind forcing for Bluelink, FOAM, and HYCOM resolves diurnal variability, but Mercator uses daily averaged winds.

Assimilation overview

Each system (Table 1) uses a different method for data assimilation. Both Bluelink and Mercator use ensemble-based schemes to represent the background error covariance – Bluelink uses Ensemble Optimal Interpolation (EnOI)^{19,20} and Mercator uses a variant of the Singular Extended Evolutive Kalman (SEK) filter.²¹ Bluelink uses a time-invariant ensemble (BODAS),⁷ and Mercator uses a seasonally-varying ensemble (SAM2).¹² Neither the Bluelink nor Mercator ensembles are state-dependent (ie, not true ensemble Kalman filters).

By contrast, both FOAM and HYCOM use an optimal interpolation approach that uses some form of analytical function to approximate the background error correlations derived from either the differences between model background fields and observations, or from model forecast fields of different lengths that are valid at the same time. The FOAM system uses the Analysis Correction (AC) approach,²² together with the so-called National Meteorological Center (NMC) approach.²³ HYCOM uses a system called NCODA, a multivariate optimal interpolation system.¹⁰

The observations assimilated by each system are quite similar (Table 1); due to continuing GODAE efforts at data assembly centres, the observations available in near-real time (NRT) for assimilation into different operational forecast systems are increasingly consistent. Bluelink does not assimilate all available observations – AMSRE is the only sea surface temperature (SST) product used by Bluelink, and Bluelink does not assimilate sea-level anomalies (SLA) from GFO. HYCOM and FOAM are the only systems that assimilate temperature data from surface drifting buoys. Bluelink and HYCOM are the only systems that do not use the First-Guess

	Bluelink/ BRAN	Bluelink/ OMAPS	UKMet/ FOAM	US NRL/ HYCOM	Mercator
Country	Australia	Australia	UK	USA	France
Model code	MOM4	MOM4	NEMO 3.0	HYCOM	NEMO 1.09
Horizontal grid	1/10°	1/10°	1/4°	1/12°	1/4°
Vertical grid	47 levels	47 levels	50 levels	32 hybrid	50 levels
Heat and freshwater fluxes	ECMWF 6h	GASP 3h	UKMO 6h	NOGAPS 1-d	ECMWF 1-d
Wind forcing	ECMWF 6h	GASP 3h	UKMO 6h	NOGAPS 3h	ECMWF 1-d
Assimilation System	BODAS	BODAS	AC/OI	NCODA	SAM2
Background error covariance	Time invariant Ensemble	Time invariant Ensemble	NMC	Flow-dependent Gaussian	Seasonally-varying Ensemble
Scheme	EnOI (120-members)	EnOI (72-members)	FOAM	MvOI	SEEK (200–220 modes)
Localising length-scale	5° GC99	8° GC99	n/a	n/a	200–500km
SST data	AMSRE	AMSRE	AVHRR + AMSRE + AATSR + <i>In-situ</i>	AVHRR + AMSRE + <i>In-situ</i>	RTG
SSH data	Jason-1 + Envisat	Jason-1 + Envisat	Jason-1 + Envisat + GFO	Jason-1 + Envisat + GFO	Jason-1 + Envisat + GFO
<i>In-situ</i>	Argo + TAO*	Argo + XBT + TAO*	Argo + XBT + buoys + TAO*	Argo + XBT + buoys + TAO*	Argo + XBT + TAO*
FGAT	No	No	Yes	No	Yes
MSL	15-yr model	15-yr model	Ri05	20-yr model	Rio05
Assimilation cycle	7-d	3-4-d	1-d	1-d	7-d
Obs window (SST/SLA/TS)	3/1/7-d	3/1/7-d	5/5/10-d	1/3/12-d	7/7/7-d
Initialisation	Nudging (1-d)	Nudging (1-d)	IAU (1-d)	IAU (6-hr)	Instantaneous update
Version	2p2	1p1	1p0	Exp 74.2	PSY3V2R2

Table 1: Summary of the model and assimilation systems for each GODAE system. All of the acronyms are either defined in the text or follow: RTG refers to Real-Time Global SST product (polar.ncep.noaa.gov/sst/); TAO* includes observations from TAO, PIRATA and RAMA; GC99 refers to Gaspari and Cohn (1999)³⁹; Rio05 refers to the MSL described by Rio and Hernandez (2004)⁴⁰

at Appropriate Time (FGAT) method, and Bluelink and Mercator do not use Incremental Analysis Updating (IAU).²⁴

Briefly, FGAT is often employed when observations from some time window, say over five days, are assimilated. When FGAT is used the model background field is compared to the observations at the observation time. So a time-varying background field is used. When FGAT is not used, it is common to compare the model background field at the analysis time, to observations over the whole time window. Also IAU relates to model initialisation. When IAU is used, the increment to the model state (the adjustment to all variables computed by the assimilation system) is added to the model field over multiple time steps. For example, if the increment is added over 10 time steps, one tenth of the increment is added at each time step – though the magnitude of the increment often varies over the initialisation period.²⁴

Products compared

The inter-comparison period spans 1 February 2008 to 15 May 2008 – Austral Summer and Autumn. The fields

provided by each group are ‘best-estimates’, plus one forecast product from Bluelink. The fields are the class 1 fields, where each group has interpolated model fields onto a common horizontal grid, for a predefined set of depths.¹⁵ Specifically, nowcasts are compared of the operational systems from the UK Met Office, hereafter referred to as UKMet; hind-casts from HYCOM (version 74.2), Mercator (version PSY3V2R2), and Bluelink (using OceanMAPS version 1p1, and BRAN version 2p2). OceanMAPS is the operational implementation of the Bluelink system,⁶ and BRAN, the Bluelink ReANalysis, is the reanalysis version²⁵. Best estimate is used from OceanMAPS, hereafter referred to as OMAPS-hc, and 3–4 day real-time forecasts from version 1p1 of OceanMAPS, hereafter referred to as OMAPS-fc.

Because OceanMAPS is initialised 5-days behind real-time, the 3–4 day forecasts reported here are the model forecasts 8–9 days after initialisation. BRAN and OceanMAPS are configured slightly differently. BRAN assimilates delayed-mode quality controlled altimetry and Argo T/S profiles but no XBT data, uses a 7-day update

cycle, using 120 ensemble members, and is forced with NRT surface fluxes from the European Centre for Medium-Range Weather Forecasts (ECMWF). By contrast, the OMPS products assimilate NRT altimeter data and Argo TS profiles plus XBT data from the Global Telecommunications System (GTS), uses a 3–4 day update cycle, using 72 ensemble members, and is forced with NRT surface fluxes from the Bureau of Meteorology’s operational NWP system (GASP).

In the next section results from each GODAE system are compared to observations and observation-based product – specifically, along-track Sea Level Anomalies (atSLA) from Jason-1, Envisat and GFO satellite altimeters; L2P AMSRE SST (www.remss.com/), surface velocities from satellite-tracked surface drifting buoys (www.aoml.noaa.gov/phod/dac), and potential temperature (T) and salinity (S) observations from the Argo program (www.argo.net), using delayed-mode Argo data where it is available (accessed from Coriolis and US GODAE in June 2009; duplicates are removed). Results from GODAE systems are also compared to observation-based analysis products. These include gridded SLA maps, produced using optimal interpolation (OI) at CSIRO (www.cmar.csiro.au/remotesensing/oceancurrents/), and a gridded SST product, also produced using OI under the Group for High Resolution SST (GHRSSST) project (www.ghrsst.org) – specifically the Regional Australian Multi-Sensor SST Analysis (RAMSSA).²⁶ Of these data, all are assimilated into each system, with the exception of the surface velocity data from drifting buoys that are only assimilated in the HYCOM system.

RESULTS AND DISCUSSION

Regions

Inter-comparisons of each system are presented here for two regions in the south-west Pacific Ocean – the East Australian

Current (EAC) region, and the Coral Sea and Papua New Guinea (PNG) region. These regions are denoted in Fig 1. The EAC region is characterised by the strong poleward currents of the EAC that flow adjacent to the east Australian coast between about 20°S and 33°S. South of about 33°S the EAC typically separates from the coast and degenerates into a complex field of mesoscale eddies.²⁵ The most salient feature of the Coral Sea is a quasi-stationary gyre, centred around 148°E and 12°S, called the North Queensland or Gulf of Papua Current²⁷. The New Guinea Coastal Current flows west-north-west along the northern coast of PNG, feeding the West Pacific warm pool²⁸. Both the EAC and the Gulf of Papua Current are fed from the westward flow of the South Equatorial Current.

Taylor diagrams

In this section, modelled and observed estimates of oceanic properties are compared using Taylor diagrams.²⁹ Taylor diagrams succinctly represent the unbiased root-mean-squared difference (ie, the RMSD after the mean has been removed) and cross-correlation between observed and modelled estimates of some quantity. Taylor diagrams also show the standard deviation of observed and model estimates. With reference to Fig 2a, showing comparisons of atSLA in the EAC region, the authors explain how Taylor diagrams can be interpreted. Taylor diagrams exploit a geometric relationship between RMSD, cross-correlation and standard deviation through the use of two over-lapping polar coordinates. Note that the mean of each estimate is removed prior to generation of the Taylor diagram, so the diagram does not provide any explicit comparison of the mean, or bias, of each estimate. The radial distance of each dot, for either a set of model estimates or observations, from the origin represents the standard deviation. Fig 2a indicates that the standard deviation of the observed atSLA is slightly greater than 0.15m. The estimate

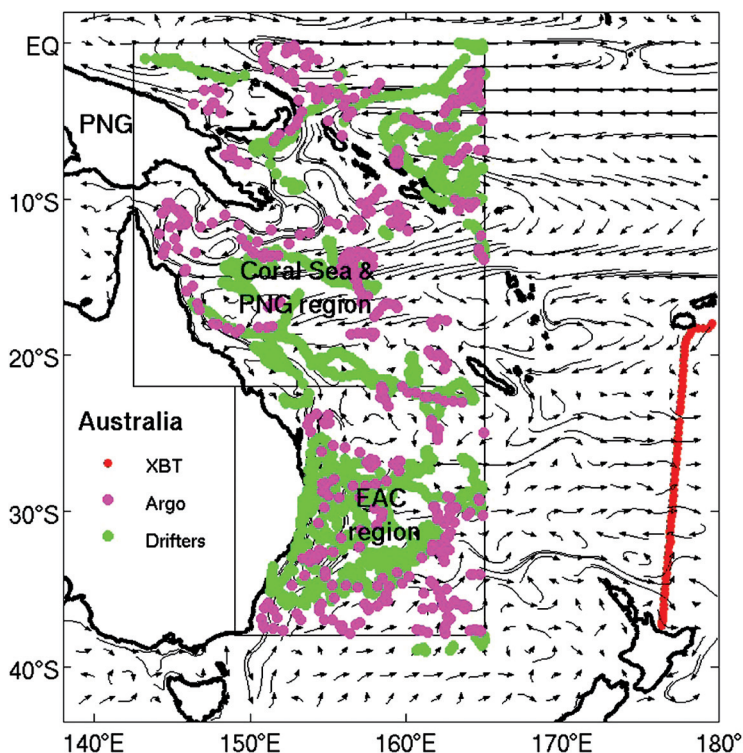


Fig 1: Map of the SW Pacific Ocean showing an estimate of the mean ocean circulation over the top 200m depth, two geographic regions (Coral Sea & PNG region; and EAC region) referred to in this study, the distribution of surface drifting buoys (green), Argo T/S profiles (magenta), and the XBT section (red)

of atSLA from BRAN, for example, is slightly less than 0.15m. The arc distance from the vertical axis corresponds to the cross-correlation between each model estimate and the observed estimate. The vertical axis corresponds to zero correlation; the horizontal axis corresponds to a correlation of 1, with an inverse cosine scaling in between. The observed dot is always along the horizontal axis because it is perfectly correlated with itself. For Fig 2a, the cross-correlation between the observed atSLA and BRAN is approximately 0.8. The distance between the dot representing the observed estimate and each model estimate is the RMSD. So Fig 2a indicates that the RMSD between the observed atSLA and BRAN is slightly less than 0.1m.

Taylor diagrams can be used to get a sense for the signal-to-noise ratio of each estimate. If the RMSD exceeds the standard deviation, the signal-to-noise is less than 1. In such a case, the model field is not quantitatively skilful because the

signal is comparable to the noise (ie, error). If the standard deviation of a model is greater than the standard deviation of the observations, then it might be concluded that the model is noisier than the observations. This might be due to unconstrained instabilities in the model, or because there is more energy in the model than in the observations – this might occur if a high resolution model is compared to a coarse resolution observation, like a Real-Time Global (RTG) SST analysis product, for example.

EAC Region

Modelled and observed estimates of atSLA, SST, and near-surface velocities in the EAC region are compared in the Taylor diagrams presented in Fig 2. Similarly, modelled and observed estimates of sub-surface T and S in the EAC region are compared in Fig 3, showing profiles of the RMSD between observed and modelled estimates. Also included in

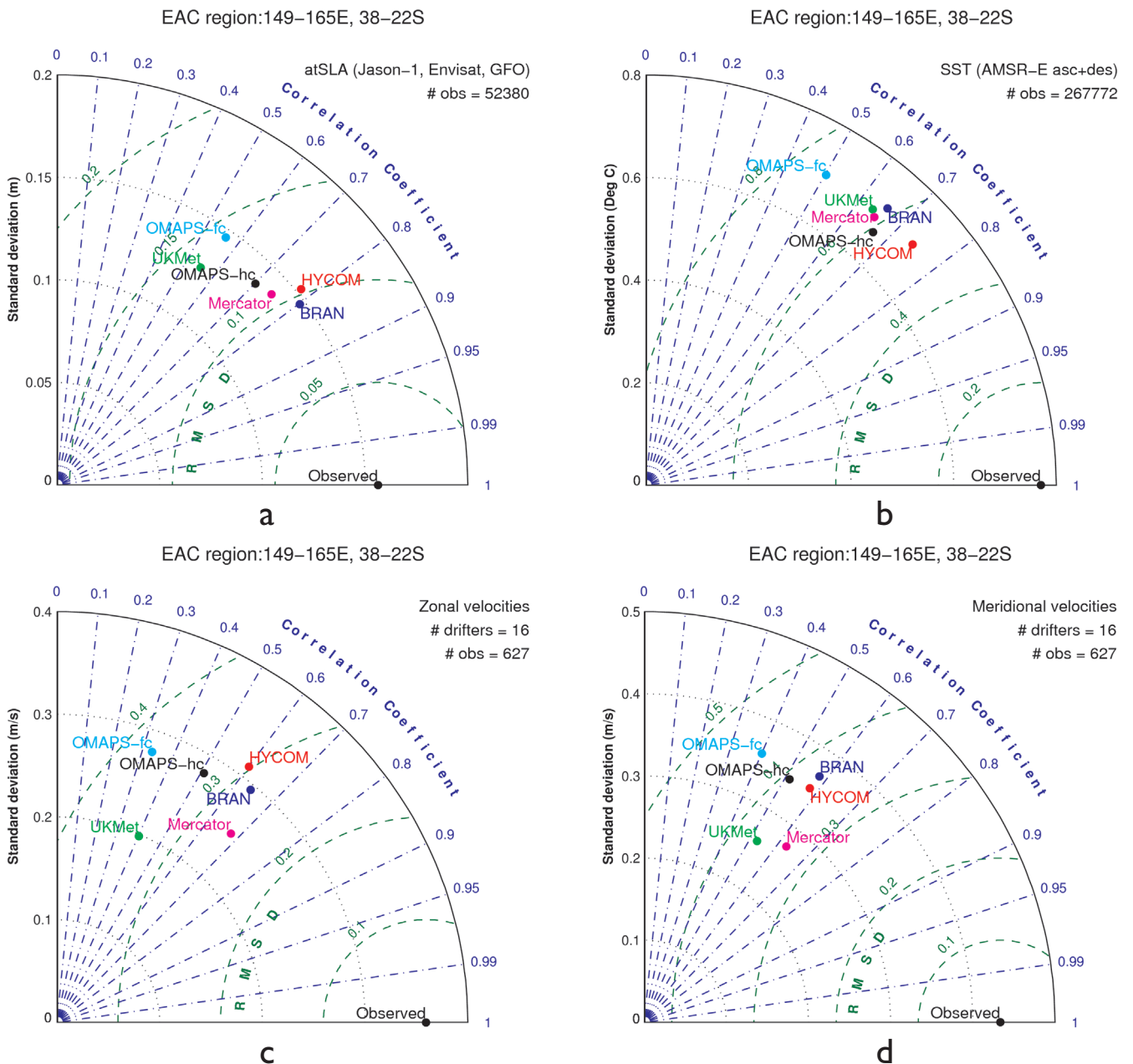


Fig 2: Taylor diagrams for (a) atSLA, (b) AMSRE SST (c) drifter-derived zonal velocities, and (d) drifter-derived meridional velocities in the EAC region. The number of observations used for each panel is listed explicitly (# obs and # drifters)

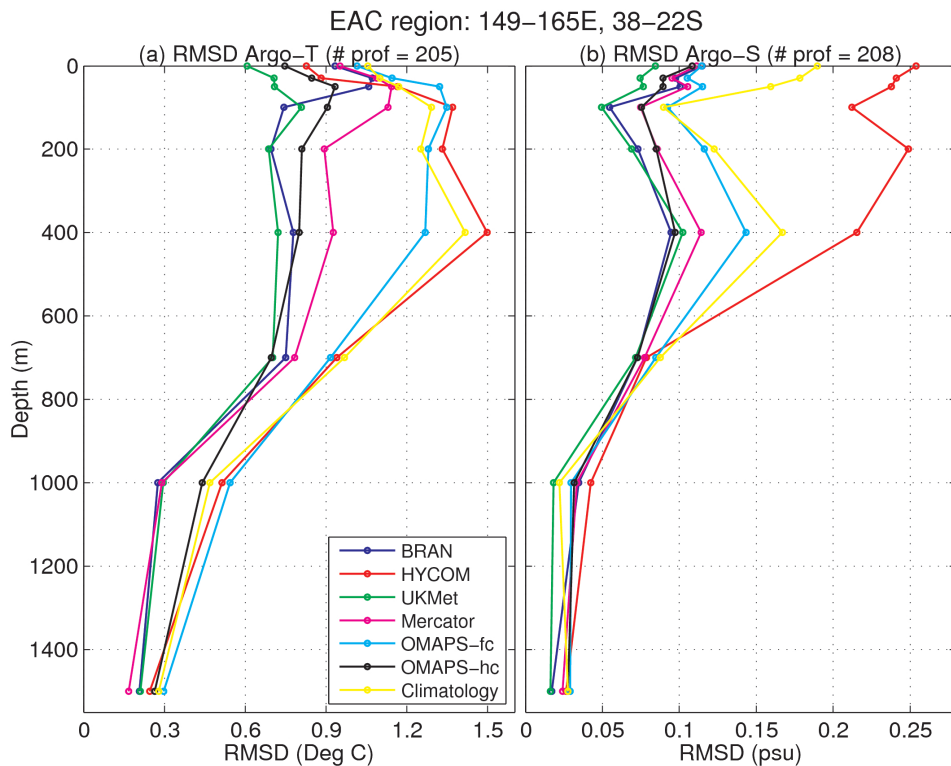


Fig 3: Profiles of the RMSD for T (left) and S (right) for each GODAE system, and for climatology, for the EAC region. The number of Argo profiles used for each panel is listed explicitly (# prof)

Fig 3 are profiles of the RMSD between observed fields and climatology (climatology from the CSIRO Atlas for Regional Seas (CARS)).³⁰

Using the RMSD as the most basic metric for evaluation, Figs 2 and 3 indicate that the model estimates closest to observations of atSLA, SST, near-surface velocity, and sub-surface T/S in the EAC come from BRAN, HYCOM, Mercator, and UKMet respectively. Both Mercator and UKMet tend to under-represent the variability of near-surface velocity, with standard deviations that are measurably less than the observations and the HYCOM and Bluelink models. This is expected, since both Mercator and UKMet models are $1/4^\circ$, that is appreciably coarser than $1/10^\circ$ and $1/12^\circ$ resolution used by Bluelink and HYCOM in this region. It is also interesting to note that UKMet tends to produce better T/S profiles compared to Mercator, while Mercator tends to produce better SLA. Noting that these systems use the same model code and grid, it is logical to conclude that these differences are attributable to the assimilation schemes that have presumably been ‘tuned’ differently for different variables – though the differences may also be related to differences in the initialisation and surface forcing.

Considering only the series of Bluelink results, the estimates from the operational forecast (OMAPS-fc) are always less skilful than the hindcast products (BRAN and OMAPS-hc), as might reasonably be expected. However, the delayed-mode reanalysis (BRAN) is *not* always more skilful than the operational hindcast product (OMAPS-hc). This may be due to the length of each update cycle – recall that BRAN assimilates observations once every 7 days, while OMAPS-hc assimilates observations once every 3 or 4 days (with twice weekly updates). It is expected that the more

frequent update cycle in OMAPS-hc translates to an improvement in the system’s performance for some variables, since instabilities in the EAC region are known to develop and evolve rapidly over very short periods, like 2–3 days. BRAN and OMAPS-hc also use different surface fluxes from operational NWP systems (see Table 1).

Considering the sub-surface profiles of the RMSD for T and S (Fig 3), the results show that, with the exception of the forecast product, all estimates have smaller errors than climatology over the upper ocean (<800m depth). This is encouraging, particularly in this region that is characterised by transient, mesoscale features. In such a region, the displacement of an eddy can result in very large RMSD statistics.⁷ Close inspection of Fig 3 near the surface seems to give a result that is somewhat inconsistent with the SST comparisons, presented in Fig 2a. Specifically, the RMSD of the near-surface T is smallest for UKMet in Fig 3a, but the RMSD of SST is smallest for HYCOM in Fig 2b. This is due to different spatial and temporal sampling of Argo (approximately 200 profiles in total for the whole region over the entire time period) and satellite SST (approximately 25km resolution maps spanning most of the region every day). This can also be attributable to the gradient in temperature in the near-surface layer and the different observing depths of *in-situ* (~1m) and satellite (microns) measurements.

Coral Sea and PNG region

Modelled and observed estimates of atSLA, SST, and near-surface velocities in the Coral Sea and PNG region are compared in the Taylor diagrams presented in Fig 4. Similarly, modelled and observed estimates of sub-surface T and S in the Coral Sea and PNG region are compared in

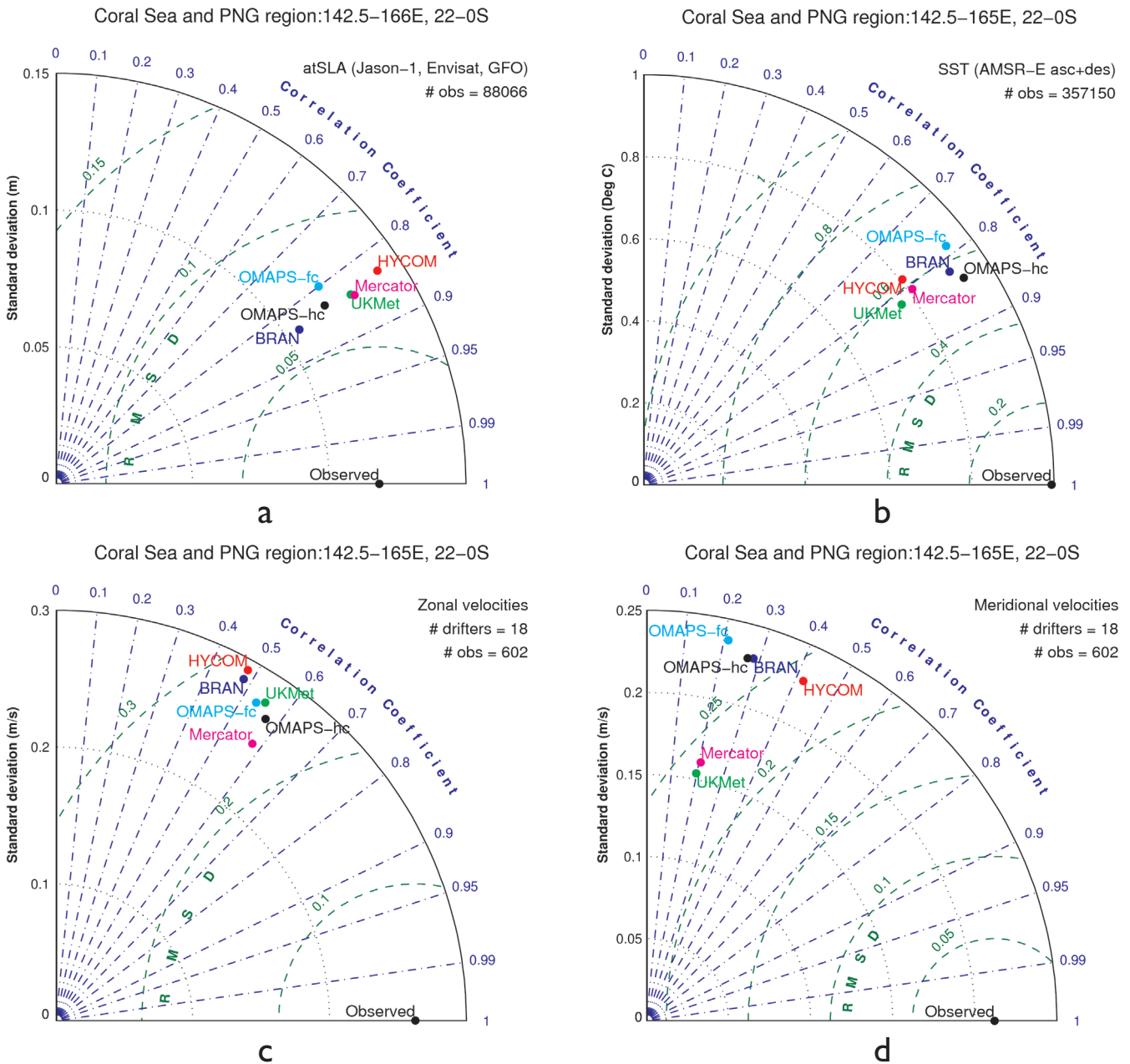


Fig 4: As for Fig 2, except for the Coral Sea and PNG region

Fig 5, showing profiles of the RMSD between observed and modelled estimates.

The RMSD statistics shown in Figs 4 and 5 again indicate that the model estimates closest to observations of atSLA, SST, near-surface velocity, and sub-surface T/S in the Coral Sea and PNG region come from BRAN, OMAPS-hc, Mercator, and UKMet respectively. For the meridional velocities, both Mercator and UKMet again tend to under-represent the variability (Fig 4d), with smaller standard deviations than the other estimates.

In this region, the RMSD between observed and modelled sub-surface T for all systems are significantly less than climatology for depths shallower than 400m – the depths that are of particular interest for GODAE systems (and indicative of the depths constrained by the remotely sensed observing system). However, the RMSD for S is not very much less than climatology. This suggests that S is not particularly well constrained by any of the models in this region – perhaps

because there are too few observations and also they are less correlated with the remotely sensed observations. It could also be an indication that the assimilation systems are generally not well tuned for S.

XBT transect

The frequently repeated XBT transect PX-6, between Auckland and Fiji (Fig 1), was occupied during the inter-comparison period. The observed T section from this line is shown in Fig 6a. Comparisons of T anomalies (ie, anomalies from CARS) at several depths, based on an agreed subset of depths,³¹ are also shown in Fig 6b-e. The RMSD between the observed and modelled T for these comparisons is shown in Table 2. These comparisons demonstrate that the GODAE models generally provide a realistic representation of the sub-surface T field. Anomalies along this section range from -1.2°C to 2.1°C ; and the GODAE systems generally represent the sign and locations of the anomalies, and the

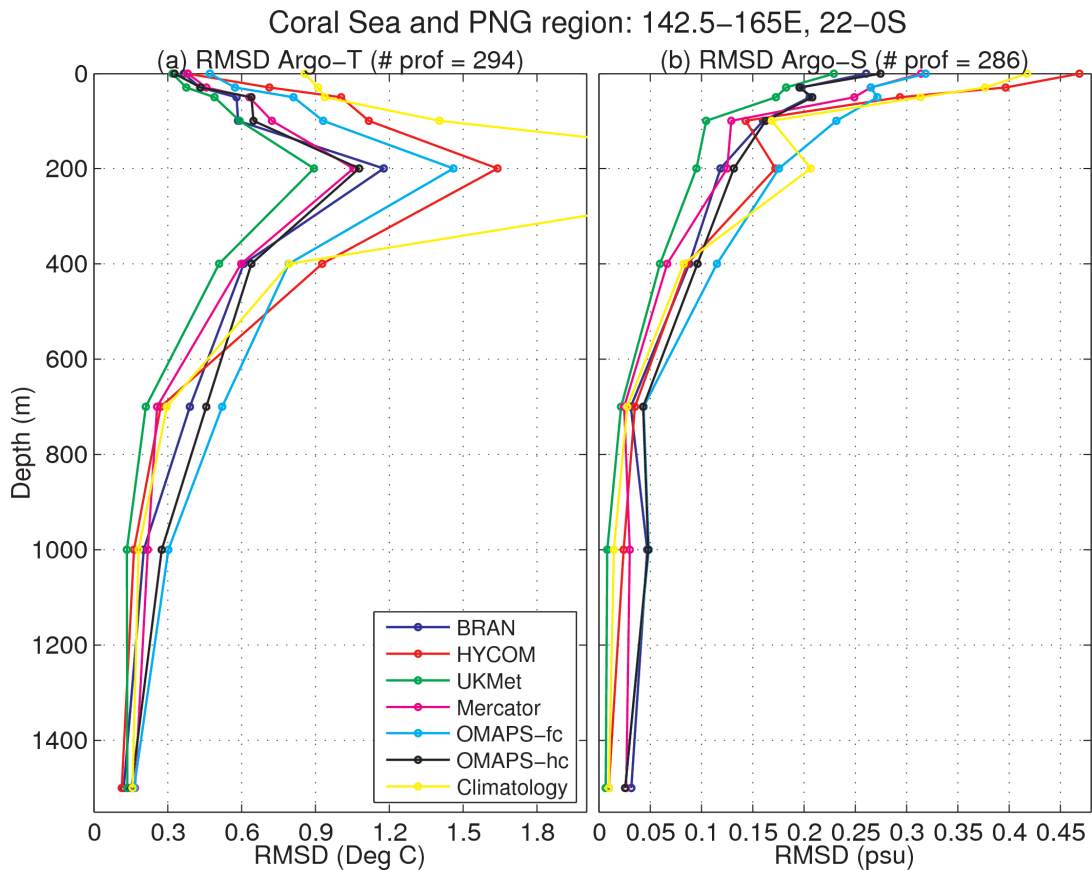


Fig 5: As for Fig 3, except for the Coral Sea and PNG region

approximate magnitude of the anomalies along the transect. Consistent with the comparisons in Figs 3 and 5, the results from UKMet, along with OMAPS-hc, appear to out-perform the others.

SLA sequence

A sequence of SLA maps are shown in Fig 7, including a model-independent analysis product as a reference that is based on optimal interpolation (labelled OI-SLA), and SLA fields from each system. The purpose of this comparison is simply to demonstrate that all systems produce realistic estimates of the time-varying state of the ocean. During the period displayed in Fig 7, the salient features include two warm-core eddies and three cold-core eddies, all in the vicinity of 31–37°S. All systems include some representation of each of these features – though their evolution over time differs. Specifically, HYCOM shows the two warm-core features being drawn together, with a hint that they will coalesce. The variability in the UKMet fields is notably less than the OI-SLA and the models. Mercator, BRAN, and OMAPS-hc all show the south-eastern-most cold-core eddy splitting into two by 26 February – a feature that is also evident in the OI-SLA, but not in HYCOM or UKmet. The differences between the models occur in the positions and intensity of mesoscale features. Notably, the performance of OMAPS-fc, the only true operational forecast product considered in this study, shows good agreement with the other products, including the OI-SLA.

SST sequence

A sequence of SST maps (Fig 8) compares a GHRSSST analysis product (RAMSSA),²⁶ with daily mean SST fields

	Depth			
	1m	50m	200m	400m
HYCOM	0.36	0.65	0.56	0.74
UKMet	0.27	0.52	0.60	0.74
BRAN	0.45	0.64	0.73	0.68
Mercator	0.32	0.65	0.58	0.61
OMAPS-fc	0.50	0.65	0.90	0.83
OMAPS-hc	0.39	0.50	0.60	0.61

Table 2: RMSD between T in each GODAE system and T along the PX-6 XBT line (with the mean difference removed in each case; see Fig 6) at various depths

from HYCOM, UKMet, Mercator, BRAN, and OMAPS. In general, all of the GODAE systems reproduce SST fields that compare well with the GHRSSST analysis. The SST fields from UKMet and Mercator are slightly smoother than GHRSSST, HYCOM, and the Bluelink products – though one could argue that they are less noisy and therefore possibly more reliable. There are times when several systems appear to have somewhat noisy SST fields. For example, note the small-scale filaments around 160°E and 35°S on 9 April in UKMet, Mercator, and BRAN. Small-scale features are also evident in GHRSSST and HYCOM – though the correspondence between those two products is very good. More generally, all model products appear to show somewhat noisy SST fields around 35°S.

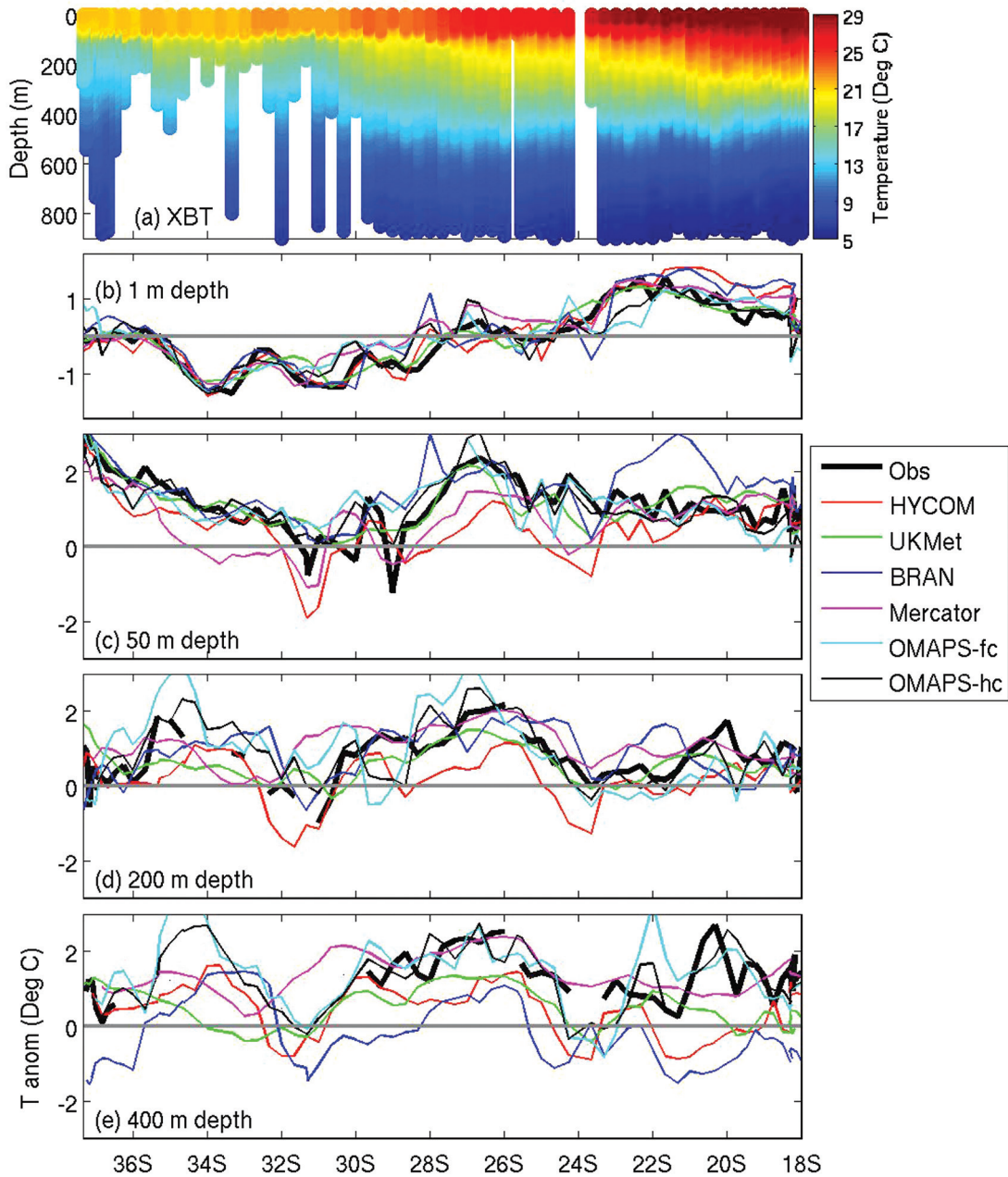


Fig 6: Comparison of T along the PX-6 XBT transect, denoted in Fig 1, that was occupied between 21–25 February 2008, showing (a) the latitude-depth section from observations, and (b–e) T anomalies (relative to climatology) from the XBT observations (bold black) and from each GODAE system (see legend) for 1, 50, 200, and 800m depth

At different times, some GODAE systems include features that appear fictitious – possibly due to assimilation of bad data, or due to dynamical instabilities in the models that are known to occur in this region³². Again, it is noted that *Bluelink* and *HYCOM* offer higher resolution than *UKMet* and *Mercator*. This might explain some of the differences. Moreover, if the *GHRSSST* product is too smooth, some SST features that appear in the high-resolution models might be absent in the *GHRSSST* product.

Variability

The standard deviation of SLA from *OI-SLA* and from each GODAE system is shown for the EAC region in Fig 9. The observation-based product (*OI-SLA*) shows six local maxima in SLA variability, with a magnitude that exceeds

0.2m. *OI-SLA* shows one local maxima around 37°S, one around 36°S (about 159°E), two around 34°S, and two around 32°S. All GODAE systems reproduce the local maxima around 37°S, all reproduce two local maxima around 34°S, and all reproduce two local maxima around 32°S. This result is very encouraging, because it demonstrates that the variability reproduced by each system is qualitatively realistic. Only *HYCOM* and *BRAN* reproduce the local maxima at 36°S; and only *Mercator* and *BRAN* realistically reproduce the magnitude of the largest maximum (at 34°S, 155°E). It is also noted that the reproduction of many of these features by *OMAPS-fc* is good. This demonstrates that the GODAE systems can realistically forecast (both persist, or maintain after initialisation, and dynamically evolve) this variability.

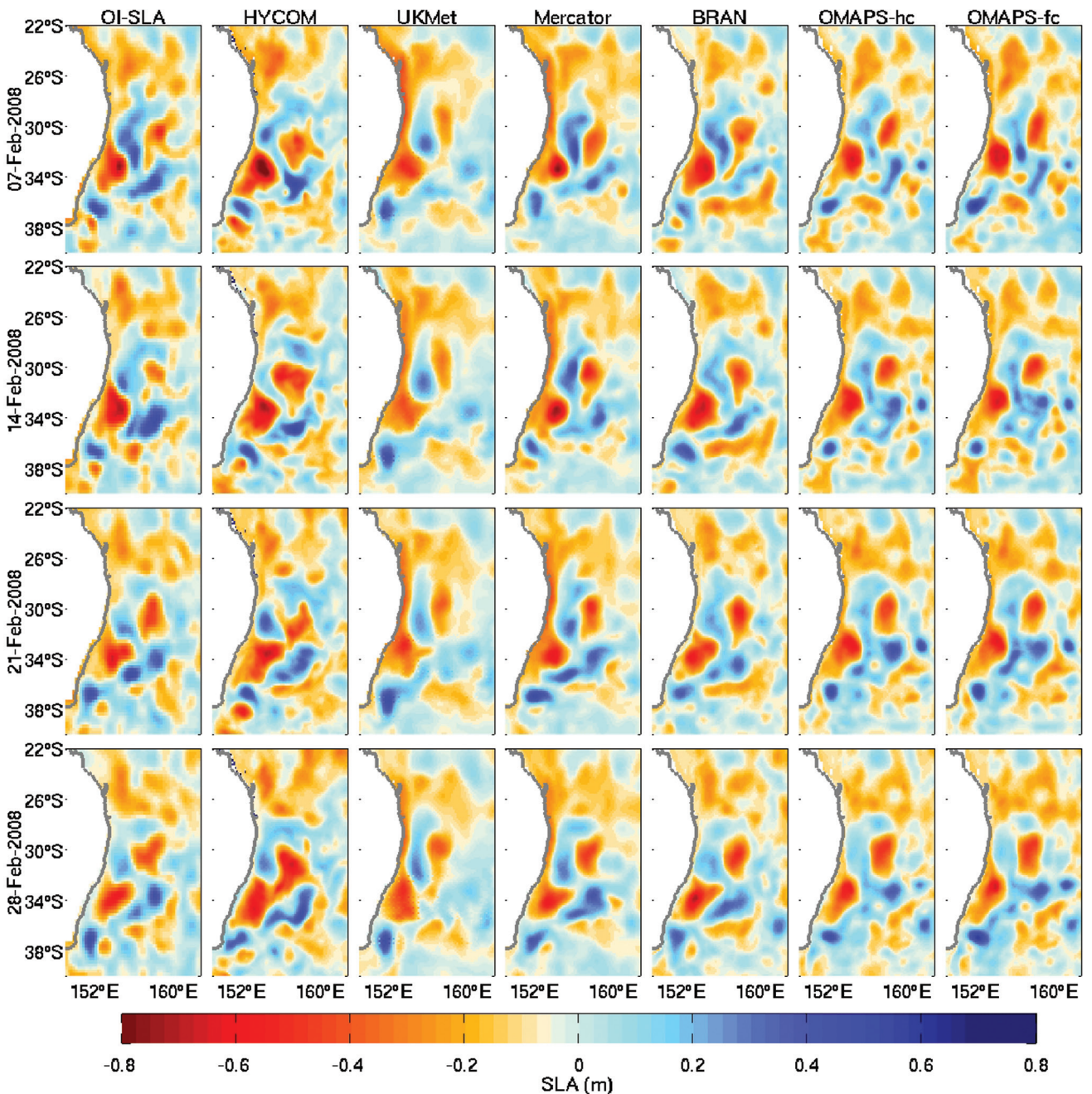


Fig 7: Sequence of daily averaged SLA during February 2008 from optimally interpolated observations (OI-SLA; col 1), and each GODAE system (cols 2–7)

The standard deviation of SST from the GHRSSST product and from each GODAE system is shown for the south-west Pacific in Fig 10. In general the GHRSSST product has lower variability than all of the GODAE systems. The most prominent feature in the observation-based product (GHRSSST) is the diagonally oriented maximum centred on about 155°E and 35°S. All of the GODAE systems reproduce a similar maximum. Another prominent feature is the band of high variability around 22°S that extends along the north-east coastal of Australia, to about 15°S.

All GODAE systems reproduce relatively high variability in these regions, though the models (with the exception of OMAPS-hc and OMAPS-fc) tend to have greater variability there, particularly near the coast, over the Great Barrier Reef (GBR). BRAN also significantly over-estimates the SST variability in Bass Strait, around 40°S. The over-estimate of SST

variability in these coastal regions (Bass Strait and GBR) is an indication that the models are less constrained and possibly lack some important physical processes (eg, tidal mixing – none of the systems considered include tides). Also, the models may be overly sensitive to the quality of the atmospheric fluxes. BRAN, for example, only assimilates AMSR-E SST that is not available within about 50km of the coast, and has no data in Bass Strait (at least none that are assimilated into BRAN). The modelled SST can show higher variability and frequency near the coast due to strong local wind forcing, and in the absence of sufficient observations, the modelled variability can become somewhat unreliable. In those locations, the accuracy of the model is closely related to the accuracy of the local wind forcing. This was shown to be true for BRAN.⁷

In general, the SST standard deviation in the models tend to be on small scales and quite noisy in the southern part

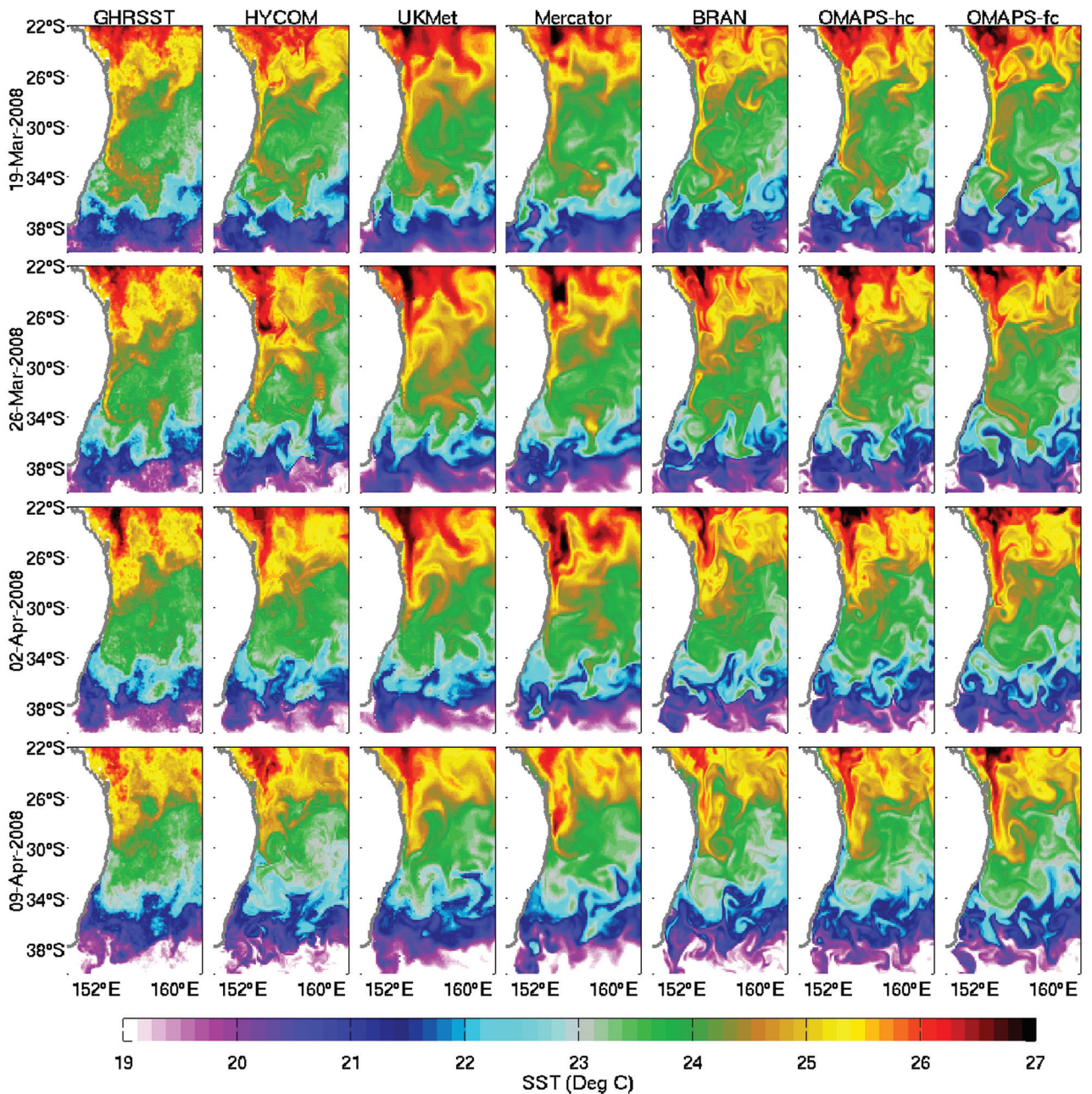


Fig 8: Sequence of daily averaged SST during March and April 2008 from a GHRSSST analysis (col 1) (RAMSSA³¹), and each GODAE system (cols 2–7)

of the domain shown in Fig 10. This is an indication of the dynamic nature of the variability there, and may imply that predictability in that region is limited by dynamic instabilities.³² Another region of interest where there is notable disagreement with observations is on the coastal side of the Gulf of Papua Current (around 10°S). All models show relatively high SST variability there (Fig 10), but the observations do not. The reason for this is unclear, but again, it may be an indication that the models are insufficiently constrained there due to a paucity of observations.

CONCLUSIONS

The purpose of this paper is to document the performance of GODAE systems at the end of the GODAE project, in 2008, and to extend the inter-comparisons¹⁵ to the Australian

region, and to include inter-comparisons with the Australian system. Comparisons between observations and GODAE systems demonstrate that each system has certain strengths and weaknesses. Inter-comparisons are regarded as valuable exercises that provide important insights into the ocean forecast systems for both developers and users. This inter-comparison study, and that of¹⁵, is one of the first attempts at performing GODAE inter-comparisons. Now that the tools have been developed, the metrics have been defined, and the community has engaged in inter-comparisons, the GODAE OceanView community is well placed to undertake more comprehensive inter-comparisons, using more complete datasets; and more compatible datasets; including class 2, 3 and 4 metrics to assess predictive skill; and on the capacity for GODAE systems to deliver forecasts that are reliably skilful delivering real benefit the user community.

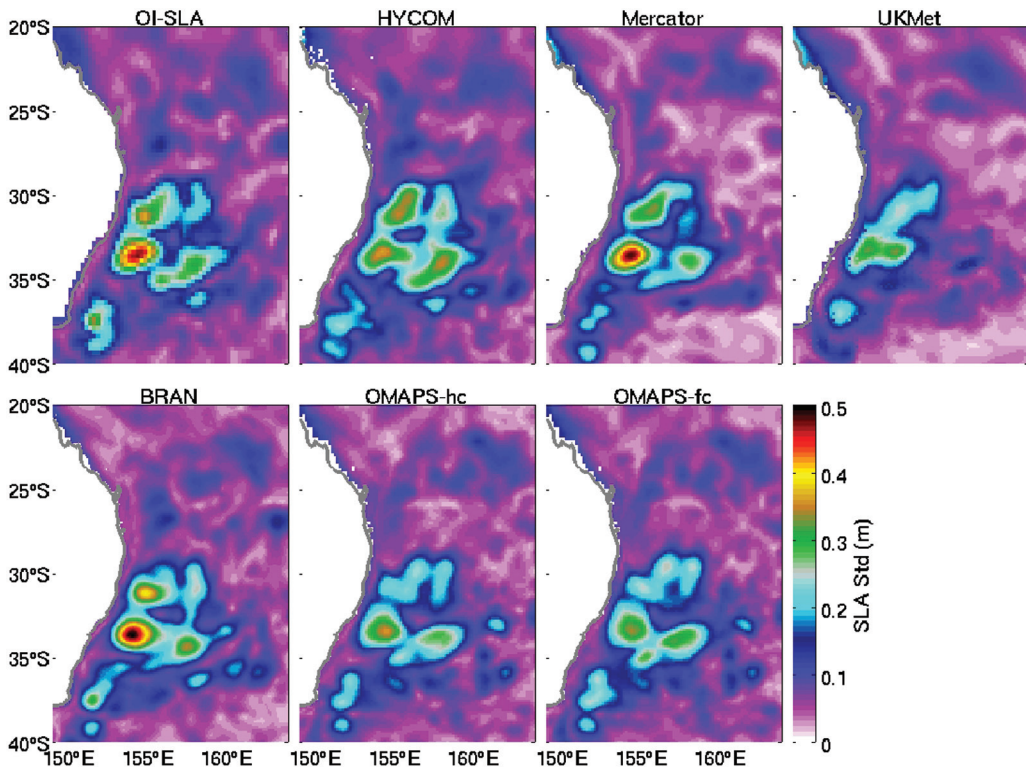


Fig 9: Standard deviation of SLA from optimally interpolated at SLA (OI-SLA) and each GODAE product

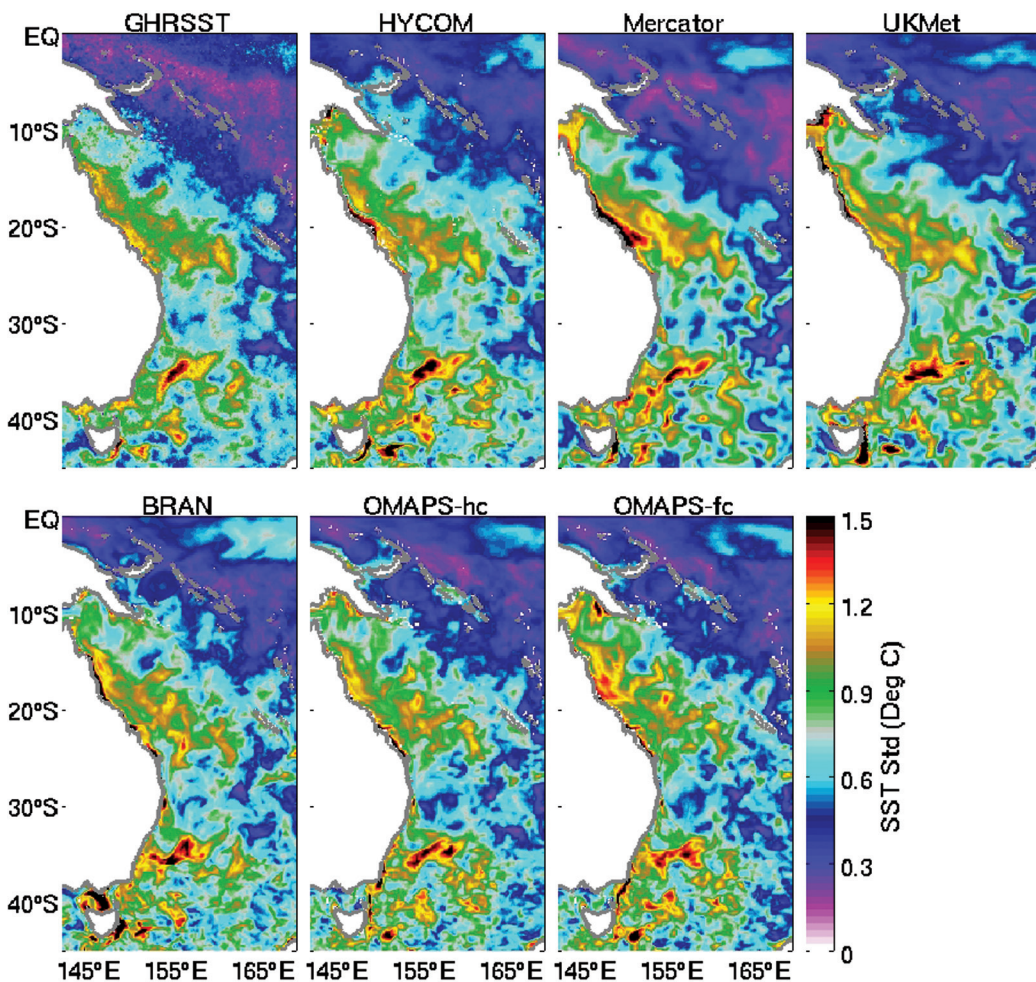


Fig 10: Standard deviation of SST from a GHRSSST analysis and each GODAE product

It is concluded that off the east coast of Australia, the Bluelink (Australian) system produces the most accurate representation of SLA, the HYCOM (USA) system produces the most accurate representation of SST, the Mercator (French) system produces the most accurate representation of near-surface velocity, and the FOAM (UKMet) system produces the most accurate representation of sub-surface T and S.

Different variables are important for different applications. So, based on this study a user might benefit from using analyses from the system with strengths in the variable most relevant to their application. For example, during a search and rescue operation, a user might adopt Mercator; to identify the position of an eddy, say for a fisheries application, a user might adopt Bluelink (BRAN); to monitor the chance of a warming event that might impact corals or aquaculture, a user might adopt HYCOM or Bluelink (OMAPS); and to predict underwater acoustics that depend strongly on sub-surface T, a user might adopt UKMet.

However, noting that the system with lowest error of the analysis or forecast for individual events varies with time (ie, the systems contain independent information), a more robust approach is to combine information from all systems together, in the form of a so-called super ensemble.³³ or a consensus forecast. Given their different strengths and weaknesses, such an ensemble could prove most useful for communities that depend on operational oceanography. This approach becomes more practical when considering the non-stationary nature of operational ocean forecasting with regular system update cycles (noted below) as well as changes to the observing system and atmospheric forcing. It is also noted that user-oriented inter-comparison studies^{34,35} should also be performed to comprehensively assess the suitability of GODAE systems for different applications.

Development of the GODAE systems used here continues under GODAE OceanView, the successor to GODAE, and the performance of each system continues to improve^{25,36,37,38} (see also the GODAE OceanView national reports at www.godae.org/documents.htm and www.godae-oceanview.org/documents/). Based on the results of this study, however, it is clear that operational oceanography is indeed feasible, and is now in full swing at several agencies. The transition of these systems into operational services is being aided through the WMO/IOC Joint Technical Commission for Oceanography and Marine Meteorology – JCOMM (www.jcomm.info). As the skill of operational systems improve through adoption of new observing systems, improvements to assimilation methods, and more accurate models, the impact of GODAE systems on industry groups and marine users is likely to continue to increase; and through the continued cooperation of international partners under GODAE OceanView, the potential to produce accurate, reliable ocean forecasts is being realised.

ACKNOWLEDGEMENTS

The following organisations and agencies are acknowledged for their financial support: European Space Agency; French Service Hydrographique Océanographique de la Marine (SHOM); Office of Naval Research; and the Royal Australian Navy. Satellite altimetry is provided by NASA, NOAA, ESA and CNES. Drifter data are provided by NOAA-AOML and

SST observations are provided by NASA, NOAA and Remote Sensing Systems. Argo data were collected and made freely available by the International Argo Project and the national programmes that contribute to it (www.argo.net). Inter-comparison studies were financed at Mercator Ocean through the funding of the European Union MERSEA Integrated Project (Contract no. SIP3-CT-2003-502885). We thank M Drévillon and C Regnier at Mercator Ocean for their contribution in preparing Mercator simulations and GODAE metrics.

REFERENCES

1. Smith NR. 2000. *The global ocean data assimilation experiment*. *Adv. Space Res.*, **25**, 1089–1098.
2. Le Traon PY, Reinecker M, Smith NR, Baharel P, Bell M, Hurlburt H and Dandin P. 2001. *Operational oceanography and prediction: a GODAE perspective*. In: Koblinsky CJ, Smith NR, (eds.) *Observing the Oceans in the 21st Century*, GODAE Project Office. Bureau of Meteorology, Melbourne, pp529–545.
3. Cummings JA, Bertino L, Brasseur P, Fukumori I, Kamachi M, Martin M, Mogensen K, Oke PR, Emmanuel C, Testut C-E, Verron J and Weaver A. 2009. *Ocean data assimilation systems for GODAE*. *Oceanography*, **22**, 102–115.
4. Dombrowsky E, Bertino L, Brassington GB, Chassignet EP, Davidson F, Hurlburt HE, Kamachi M, Lee T, Martin MJ, Mei S and Tonani M. 2009. *GODAE systems in operation*. *Oceanography*, **22**, 80–95.
5. Oke PR, Schiller A, Griffin GA and Brassington GB. 2005. *Ensemble data assimilation for an eddy-resolving ocean model*. *Quarterly Journal of the Royal Meteorological Society*, **131**, 3301–3311.
6. Brassington GB, Pugh TF, Spillman C, Schulz E, Beggs H, Schiller A and Oke PR. 2007. *BLUElink> development of operational oceanography and servicing in Australia*. *J. Res. Pract. Inf. Tech.*, **39**, 151–164.
7. Oke PR, Brassington GB, Griffin DA and Schiller A. 2008. *The Bluelink Ocean Data Assimilation System (BODAS)*. *Ocean Modelling*, **21**: 46–70.
8. Bell MJ, Forbes RM, and Hines A. 2000. *Assessment of the FOAM global data assimilation system for real-time operational ocean forecasting*. *J. Mar. Syst.*, **25**, 1–22.
9. Martin MJ, Hines A and Bell MJ. 2007. *Data assimilation in the FOAM operational short-range ocean forecasting system: a description of the scheme and its impact*. *Quarterly Journal of the Royal Meteorological Society*, **133**, 981–995.
10. Cummings JA. 2005. *Operational multivariate ocean data assimilation*. *Quart. J. Royal Met. Soc.*, **131**, 3583–3604.
11. Metzger EJ, Smedstad OM, Thoppil P, Hurlburt HE, Franklin DS, Peggion G, Shriver JF, Townsend TL and Wallcraft AJ. 2010. *Validation test report for the Global Ocean Forecast System V3.0 – 1/12° HYCOM/NCODA: Phase II*. NRL Memo. Report, NRL/MR/7320–10-9236.
12. Drévillon M, Bourdallé-Badie R, Derval C, Drillet Y, Lellouche J-M, Rémy E, Tranchant B, Benkiran M, Greiner E, Guinehut S, Verbrugge N, Garric G, Testut C-E, Laborie M, Nouel L, Baharel P, Bricaud C, Crosnier L, Dombrowsky E, Durand E, Ferry N, Hernandez F, Galloudec O Le, Messal F and Parent L. 2008. *The GODAE/Mercator-Ocean global ocean forecasting system: results, applications and prospects*. *Journal of Operational Oceanography*, **1**, 51–57.

13. Bertino L and Liseter KA. 2008. *The TOPAZ monitoring and prediction system for the Atlantic and Arctic Oceans*. *Journal of Operational Oceanography*, **2**, 15–19.
14. Kamachi M, Kurangano T, Ichikawa H, Nakamura H, Nishina A, Isobe A, Ambe D, Arai M and Gohda N. 2004. *Operational data assimilation system for the Kuroshio South of Japan: reanalysis and validation*. *J. Oceanogr.*, **60**, 303–312.
15. Hernandez F, Bertino L, Brassington GB, Chassignet E, Cummings J, Davidson F, Dréville M, Garric G, Kamachi M, Lellouche J-M, Mahdon R, Martin MJ, Ratsimandresy A and Regnier C. 2009. *Inter-comparison studies within GODAE*. *Oceanography*, **20**, 128–143.
16. Brasseur P, Bahurel P, Bertino L, Birol F, Brankart J-M, Ferry N, Losa S, Rémy E, Schröter J, Skachko S, Testut C-E, Tranchant B, van Leeuwen PJ and Verron J. 2005. *Data assimilation for marine monitoring and prediction: The Mercator operational assimilation systems and the MERSEA developments*. *Q. J. R. Met. Soc.*, **131**, 3561–3582.
17. Hurlburt HE, Brassington GB, Drillet Y, Kamachi M, Benkiran M, Bourdalle-Badi R, Chassignet EP, Jacobs GA, Le Galloudec O, Lellouche J-M, Metzgar EJ, Oke PR, T. Pugh TF, Schiller A, Smedstad OM, Tranchant B, Tsujino H, Usui N and Wallcraft AJ. 2009. *High-resolution global and basin-scale ocean analyses and forecasts*. *Oceanography*, **22**, 80–97.
18. Griffies SM, Pacanowski RC and Rosati A. 2004. A technical guide to MOM4. GFDL Ocean Group Technical Report No.5 NOAA/Geophysical Fluid Dynamics Laboratory, 371pp.
19. Oke PR, Allen JS, Miller RN, Egbert GD and Kosro PM. 2002. *Assimilation of surface velocity data into a primitive equation coastal ocean model*. *Journal of Geophysical Research*, **107**(C9), 3122–3147.
20. Evensen G. 2003. *The Ensemble Kalman Filter: theoretical formulation and practical implementation*. *Ocean Dyn.* **53**, 343–367.
21. Testut C-E, Brasseur P, Brankart J-M and Verron J. 2003. *Assimilation of sea-surface temperature and altimetric observations during 1992–1993 into an eddy permitting primitive equation model of the North Atlantic Ocean*. *J. Mar. Sys.*, **40–41**, 291–316.
22. Lorenc AC, Bell RS and MacPherson B. 1991. *The Met Office analysis correction data assimilation scheme*. *Q. J. R. Meteorol. Soc.*, **117**: 59–89.
23. Kanamitsu M. 1989. Description of the NMC global data assimilation and forecast system. *We. Forecasting*, **4**, 335–342.
24. Bloom SC, Takas LL, Da Silva AM, and Ledvina D. 1996. Data assimilation using incremental analysis updates. *Monthly Weather Review*, **124**, 1256–1271.
25. Oke PR and Griffin DA. 2011. *The cold-core eddy and strong upwelling off the coast of New South Wales in early 2007*. *Deep Sea Research*, **58**, 574–591, doi:10.1016/j.dsr2.2010.06.006.
26. Beggs H, Zhong A, Warren G, Alves O, Brassington GB and Pugh TF. 2010. RAMSSA – An operational, high-resolution, multi-sensor sea surface temperature analysis over the Australian region. Submitted.
27. Steinberg C. 2007. *Impacts of climate change on the physical oceanography of the Great Barrier Reef*. In: Climate Change and the Great Barrier Reef, Johnson JE and Marshall PA (eds), pp51–74, Great Barrier Reef Mar. Park Auth., Townsville, Queensland, Australia.
28. Cresswell GR. 2000. *Coastal currents of northern Papua New Guinea and the Sepik River outflow*. *Mar. Freshwater Res.*, **51**, 553–64, [10.1071/MF991351323-1650/00/060553](https://doi.org/10.1071/MF991351323-1650/00/060553).
29. Taylor KE. 2001. *Summarizing multiple aspects of model performance in a single diagram*. *J. Geophys. Res.*, **106**, 7183–7192.
30. Ridgway KR and Dunn JR. 2003. *Mesoscale structure of the mean East Australian current system and its relationship with topography*. *Progress in Oceanography*, **56**, 189–222.
31. Crosnier L, Le Provost C and MERSEA Strand Team. 2006. *Internal metrics definition for operational forecast systems inter-comparison: Examples in the North Atlantic and Mediterranean Sea*. pp. 455–465 in GODAE Summer School in ‘Ocean weather forecasting: An integrated view of oceanography’. Chassignet EP and Verron J, eds. Springer, Lallonde les Maures, France.
32. O’Kane TJ, Oke PR and Sandery PA. 2010. *Predicting the East Australian current*. *Ocean Modelling*, **38**, 251–266.
33. Vandenbulcke L, Beckers J-M, Lenartz F, Barth A, Poulain P-M, Aidonidis M, Meyrat J, Arduin F, Tonani M, Fratianni C, Torrisi L, Pallela D, Chiggiato J, Tudor M, Book JW, Martin P, Peggion G and Rixen M. 2009. *Super-ensemble techniques: Application to surface drift prediction*. *Progress in Oceanography*, **82**, 149–167.
34. Hackett B, Comerma E, Daniel P and Ichikawa H. 2009. *Marine oil pollution prediction*. *Oceanography*, **22**, 168–175.
35. Davidson FJM, Allen A, Brassington GB, Brevik O, Daniel P, Kamachi M, Sato S, King B, Lefevre F, Sutton M and Kaneko H. 2009. *Applications of GODAE ocean current forecasts to search and rescue and ship routing*. *Oceanography*, **22**, 176–181.
36. Storkey D, Blockley EW, Furner R, Giuavarc’h C, Lea D, Martin MJ, Barciela RM, Hines A, Hyder P and Siddorn JR. 2010. *Forecasting the ocean state using NEMO: The new FOAM system*. *J. Operational Oceanography*, **3**, 3–15.
37. Ferry M, Parent L, Garric G, Barnier B and Jourdin NC. *Mercator ocean team (2010) Mercator global eddy permitting ocean reanalysis GLORYS1V1: Description and Results*. *Mercator Ocean Quarterly Newsletter*, **36**, 15–27.
38. Brassington GB, Freeman J, Huang X, Pugh T, Oke PR, Sandery PA, Taylor A, Andreu-Burillo I, Schiller A, Griffin DA, Fiedler R, Mansbridge J, Beggs H and Spillman CM. 2012. *Ocean Model, Analysis and Prediction System (OceanMAPS): version 2*. CAWCR Technical Report No.052, pp120. (www.cawcr.gov.au/publications/technical-reports/CTR_052.pdf).
39. Gaspari G and Cohn SE. 1999. *Construction of correlation functions in two and three dimensions*. *Quart. J. R. Meteor. Soc.* **125**, 723–757.
40. Rio M-H and Hernandez F. 2004. *A mean dynamic topography computed over the world ocean from altimetry, in-situ measurements, and a geoid model*. *J. Geophys. Res.*, **109**, C12032.